<論 文>

Monthly Wind Stress and Wind Stress Curl Distributions in the Easten Sea(Japan Sea)

東海上의 月別 바람應力 및 바람應力컬 分布

金 哲 鎬*
Kim, Cheol ho
崔 秉 昊**
Choi, Byung ho

要 旨

東海上의 觀測風速資料와 大氣壓資料를 各己 根據하여 月別 바람應力, 바람應力컬 및 海水體積輸送 흐름函數를 算定하였다. 두 方法에 의한 算定結果는 地域的, 季節的인 差가 있었으며 共通的인 樣相은 冬季 北西季節風에 의한 南東向의 바람應力과 夏季의 南風에 대한 北向, 北東向의 바람應力 및 冬季의 東海北部에서의 강한 反時計方向的 컬이다.

海面氣壓資料로부터 算定된 分布에서는 局地的으로 바람應力의 最大値 및 小規模의 컬들이 시베리아南東沿岸 및 우리나라 北東沿岸에서 提示되었다. Sverdrup 式으로부터 算定한 體積輸送의 分布는 우리나라 東海岸을 따라 冬季의 強한 境界流와 夏季의 弱한 南向의 境界流가 發生할 수 있음을 示唆하고 있다.

Abstract

Monthly wind stress, wind stress curl and volume transport stream functions are computed in the Eastern Sea(Japan Sea) based upon observed wind and atmospheric pressure data respectively. The presented two results show different distributions on locality and season but as common features the results reveal the northwesterly surface wind stress due to the monsoon in winter, south to southwesterly wind stress due to the southerly wind in summer and strong anticyclonic curl in the northern part on the Eastern Sea(Japan Sea) in winter.

In the distributions obtained from the sea level atmospheric pressure data, the maximum value of the wind stress and of curls of small scales are shown off the southeast coast of Siberia and northeast coast of Korea. Volume transport distributions obtained from the Sverdrup relationship suggest that the strong northward boundary current can be formed along the northeast coast of Korea in winter and weak southward boundary current in summer.

* Department of Oceanography, Seoul National University, Seoul 151, Korea
** Department of Civil Engineering, Sung Kyun Kwan University, Suwon Campus, Suwon 170, Korea

INTRODUCTION

In the investigation of the general ocean circulation an attention has been paid to the global distribution of the wind stress field for its role of forcing the upper layer ocean as the major force among the various forces. The results of the theoretical works initiated by Sverdrup(1947) and developed by Stommel(1948), Munk(1950) and others have shown that a great deal of mass transports in the ocean can be explained as those transported by wind. In the numerical experiments such as Bryan(1963) and Bryan and Cox(1967) it was reported that the different form of wind stress field had changed the circulation pattern in the ocean.

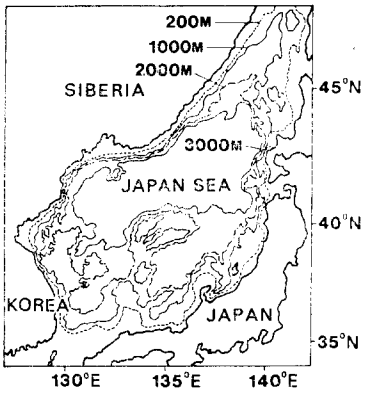

Fig. 1. The bottom topography of the Eastern Sea(Japan Sea).

As for the Japan Sea which is a marginal sea of the Pacific Ocean with the length scale of more than 10° to the north-south direction (Fig. 1), it is supposed that the circulation is driven not only by the inflow of the Tsushima Current through the Korea Strait but also by the wind, especially by the strong northwesterly wind in winter. However past studies on the mass transports and circulation dynamics (Kawabe, 1982; Yoon, 1982) have been focused mainly on the southern inflow region of the Japan Sea, it is still a question how the overall circulation pattern is in the Japan Sea. Therefore, to investigate the circulation in the Japan Sea not only the regular and dense hydrographic observations but also the informations on the wind stress data are required over the whole Japan Sea.

On the global distribution of wind stress and wind stress curl Stommel(1965) has presented an annual mean chart of the surface stress curl and Hellerman(1967) has compiled the seasonal and annual wind stress of world ocean. Based on Hellerman(1967)'s data Hantel(1971) has shown the global distribution of seasonal and annual mean wind stress curl. Evenson and Veronis(1975) have also presented continuous distribution of wind stress and stress curl by the spline function interpolation method using the same Hellerman's data. Recently Han and Lee (1981) (hereafter refer to as H&L) have updated monthly and annual mean wind stress curl with the observed wind data which have been accumulated in the U.S. National Climatic Center.

From the previously mentioned maps and charts it is difficult to get the detailed wind stress information on the Japan Sea because the resolution is very low around the marginal seas of the ocean. Among those investigators, however, H&L provide wind stress values on relatively denser grid points in the Japan Sea.

As Evenson and Veronis(1975) have already pointed out, it is obvious that the interpolated values to a smaller scale can yield no more meaningful structure than that of the observed values. To complete this deficiency, we first interpolated the wind stress from H&L's presentation and then carried out another method, that is, deduction of the surface wind and wind stress from the atmospheric pressure data. In this paper the results from the two methods about wind stress, wind stress curl and volume transports obtained depending upon Sverdrup relationship are presented and discussed.

Present analysis is attempted as an initial study of the associated programme on investigating the circulation in the Japan Sea.

METHOD OF CALCULATION

H&L's monthly mean wind stress data are provided on a $5° \times 5°$ global grid(denoted by × in Fig.2). With the basic assumption that the wind speed for any direction can be closely approximated by a Gaussian distribution,

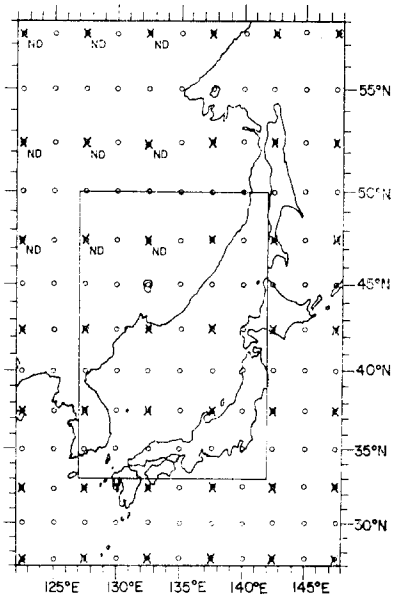

Fig. 2. Grid systems for the computation of wind stress. Open circles denote input points of atmospheric pressure and crosses input points of wind stress presented by Han and Lee(1981). ND refers grid points where wind stress values are not available.

they treated speed and direction statistically for each category. The wind stress values provided from H&L are linearly interpolated on a $1°\times1°$ grid system of which the coverage is from 27.5°N to 57.5°N latitude, from 122.5°E to 147.5°E longitude(Fig. 2). The interpolated wind stress values are reinterpolated on a $0.25°\times0.25°$ small grid system with the scale of 33°N-50°N latitude, 127°E-142°E longitude(Fig. 2).

The sea level atmospheric pressure data were provided from the Japan Meteorological Agency(1968), who has compiled the monthly mean sea level global atmospheric pressure data averaged during the period of 55 years from 1881 to 1935. The pressure data presented on a $2.5°\times2.5°$ global grid(denoted by O in Fig. 2) are interpolated on a $1°\times1°$ grid system which is the same as that used in the former calculation. From the pressure gradients components of geostrophic wind are deduced by employing the well-known geostrophic equation. Surface wind is obtained from the previously calculated geostrophic wind depending on the following empirical formula(Hasse and Wagner(1971))

$$W=aW_g+b \quad \cdots\cdots(1)$$

where, W, W_g denote surface and geostrophic wind speed in meter per second and a, b constants depending upon latitude and stability condition which are shown in Table 1. In the present study linearly interpolated values of a and b are used every 1° latitude from those values in Table 1. The stability condition is determined

Table 1. Variation of linear surface and geostrophic wind relationship

Lititude	30°N	40°N	50°N	Stability ($t_{air}-t_{sea}$)
Slope a	0.38	0.47	0.54	
Constant term	4.0	3.5	3.1	unstable (≤ -2.7°C)
b(msec^{-1})	3.2	2.8	2.5	near-neutral (-0.2°C)
	1.9	1.7	1.6	stable ($\geq +1.7$°C)

by air-sea temperature difference following the Hasse and Wagner(1971)'s criteria. Monthly mean values of air-sea temperature difference were obtained from the Japan Meteorological Agency(1972). Since the spatial variation of the air-sea temperature difference roughly falls into the single stability range, the stability of the whole study area can be classified definitely in each month. The classified unstable months are January, February, March, November, December and annual mean condition. Other months are classified as neutral. The angular deviation of the surface wind from the geostrophic wind is assumed to be 20°.

Next the wind stress is calculated from the quadratic law

$$\tau=\mathrm{Cd}\ \rho_a|W|W \quad \cdots\cdots(2)$$

where ρ_a is the air density which is taken as 0.00125 gr cm^{-3} and Cd the drag coefficient proposed by Heaps (1965).

From the wind stress obtained from equation (2), the normal component of the wind stress curl to the sea surface is calculated by finite difference form of the following equation

$$k\cdot\nabla\times\tau=\frac{1}{R\cos\phi}\frac{\partial\tau_\phi}{\partial\lambda}-\frac{1}{R}\frac{\partial\tau_\lambda}{\partial\phi}+\frac{\tau_\lambda}{R}\tan\phi \quad \cdots\cdots(3)$$

where R is the radius of the earth, ϕ is latitude, and λ is longitude; τ_ϕ is meridional component of wind stress and τ_λ zonal component.

The Sverdrup transport relationship

$$\frac{2\Omega\cos\phi}{R}M_\phi=\frac{1}{\rho}\vec{k}\cdot\nabla\times\tau \quad \cdots\cdots(4)$$

and

$$\frac{\partial_\phi}{\partial_\lambda}=RM_\phi\cos\phi \quad \cdots\cdots(5)$$

are used to obtain the meridional volume transport M_ϕ and the volume transport stream function ϕ. In the above equation, Ω is the angular velocity of the earth's rotation and ρ is sea water density. The volume transport stream function at each longitude can be obtained by integrating the term $\partial_\phi/\partial_\lambda$ westward from the eastern boundary of the Japan Sea.

REPRESENTATION OF WIND STRESS, WIND STRESS CURL AND VOLUME TRANSPORT STREAM FUNCTION

Wind stress

The interpolated wind stress distributions from H&L's data and the deduced wind stress distributions from atmospheric pressure are displayed in Fig. 3, Fig. 4 and Fig. 5, respectively. Some of the main features are as follows.

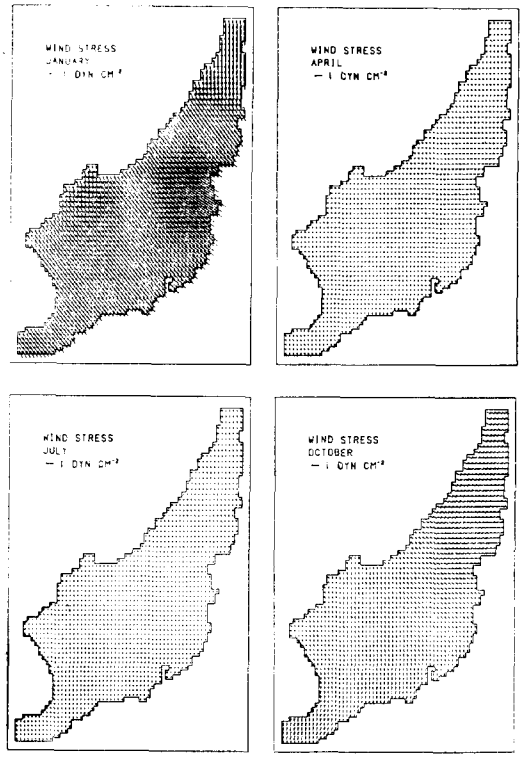

Fig. 3. Wind stress over the Japan Sea interpolated from the data of Han and Lee(1981).

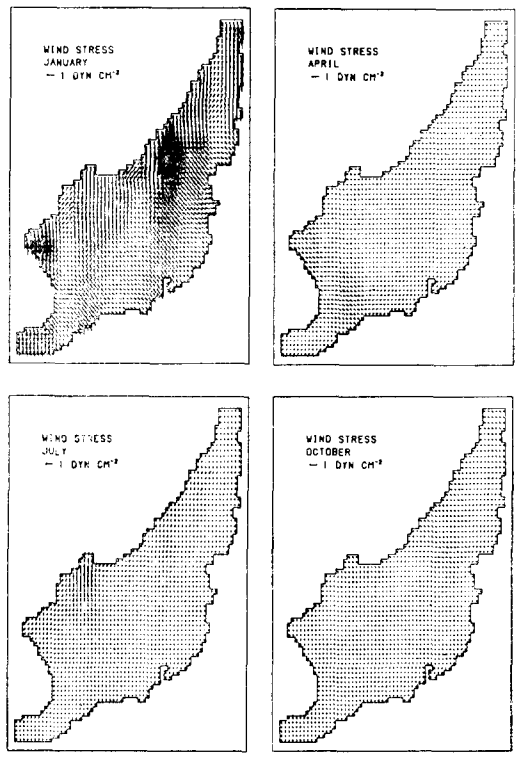

Fig. 4. Wind stress over the Japan Sea computed from the atmospheric pressure.

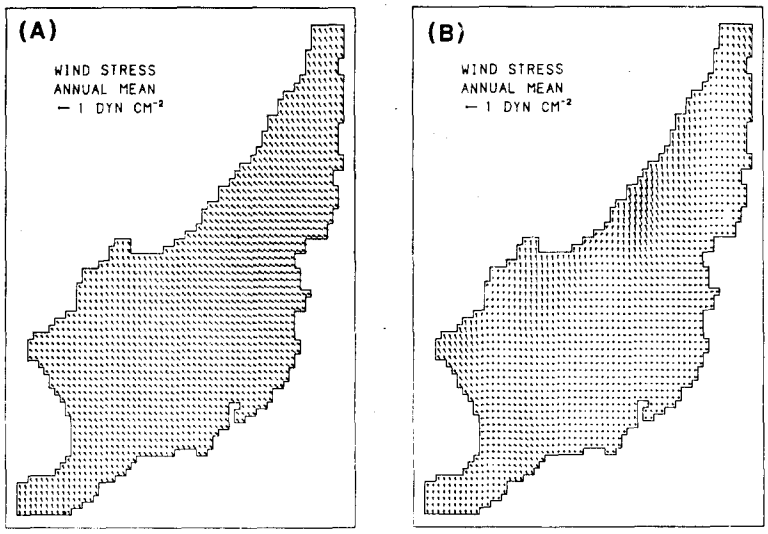

Fig. 5. Annual mean wind stress over the Japan Sea. (a) Interpolated from the values presented by Han and Lee(1981). (b) Computed from the atmospheric pressure.

(1) From the two sets of distributions it is commonly shown that the wind stress is directed southeast due to the dominant northwesterly wind from October to March next year and weakly north to northeast due to the southwesterly wind from April to September(Fig. 3 and Fig. 4).

(2) The magnitude of the wind stress obtained from H&L's data is of the order of 1.0 dyn cm^{-2} in January and becomes almost negligible in July(Fig. 3). The annual mean is of the order of 0.5 dyn cm^{-2}(Fig. 5). But in the distribution computed from the atmospheric pressure the maximum value of up to 3.5 dyn cm^{-2} is shown off the southeast coast of Siberia and in the Gulf of Yeongheung in January(Fig. 4).

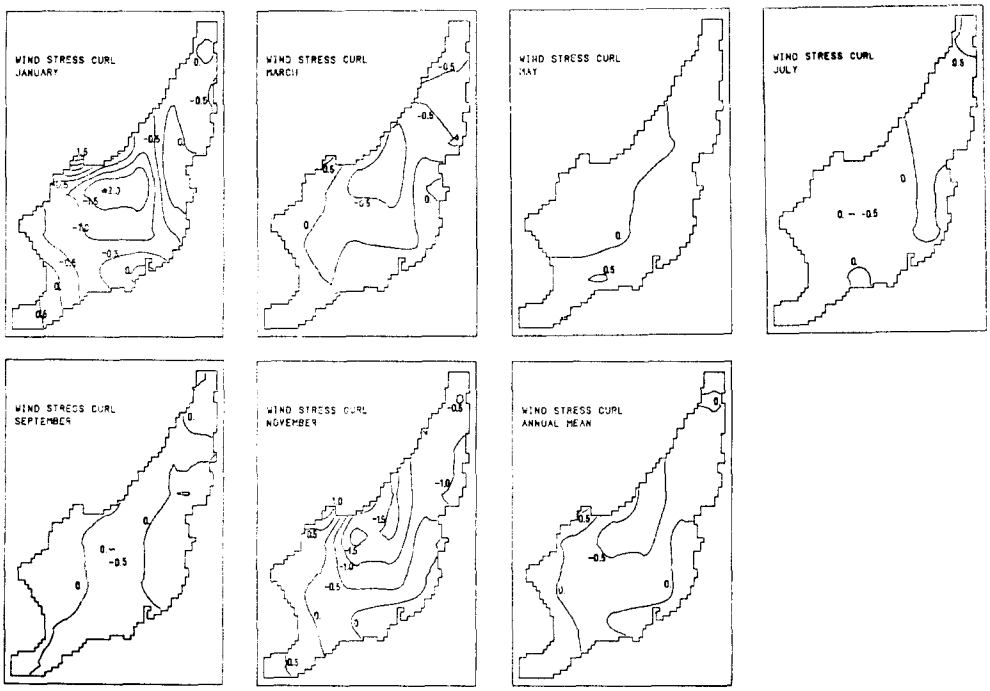

Fig. 6. Wind stress curl over the Japan Sea computed from the wind stress given by Han and Lee(1981). Contour units are 10^{-8} dyn cm^{-3}.

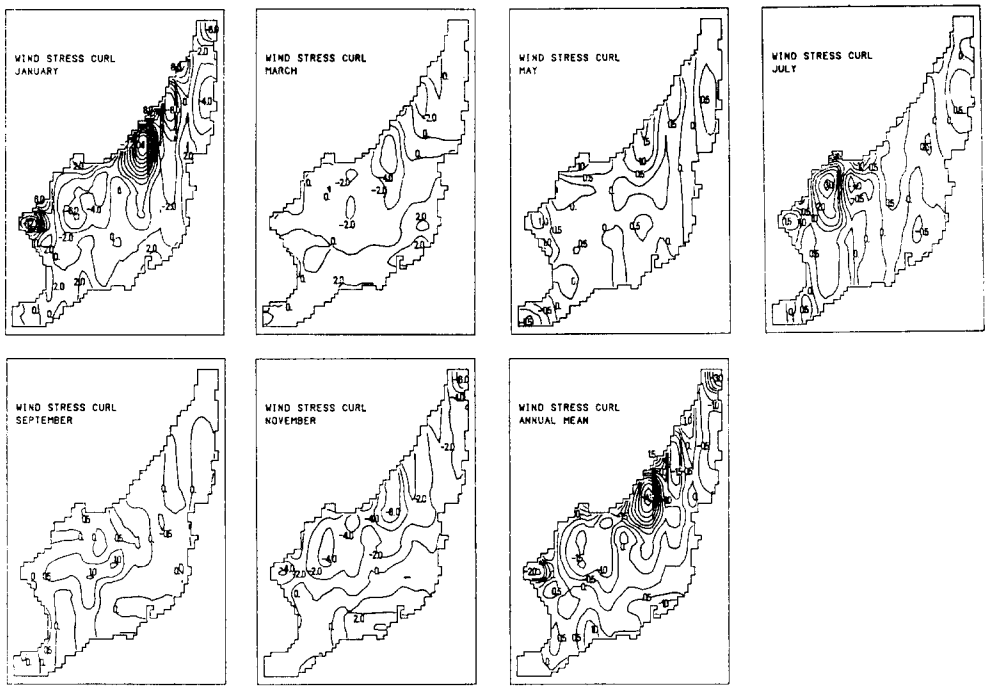

Fig. 7. Wind stress curl over the Japan Sea computed from the atmospheric pressure. Contour units are 10^{-8} dyn cm^{-3}.

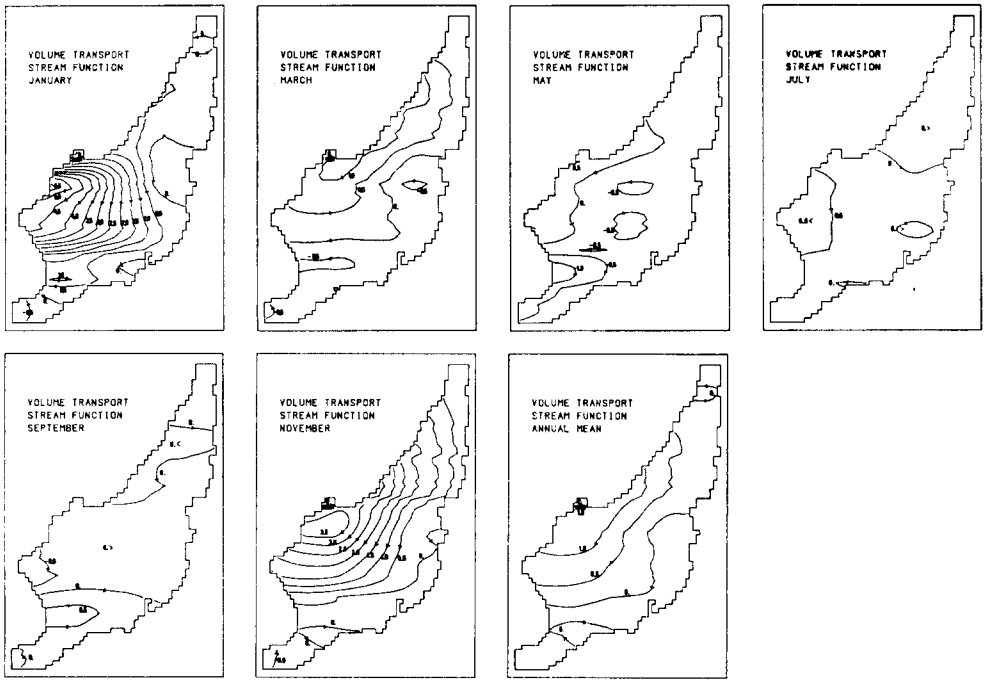

Fig. 8. Volume transport stream function over the Japan Sea computed from the wind stress presented by Han and Lee(1981). Contour units are 10^6 m^3 sec^{-1}.

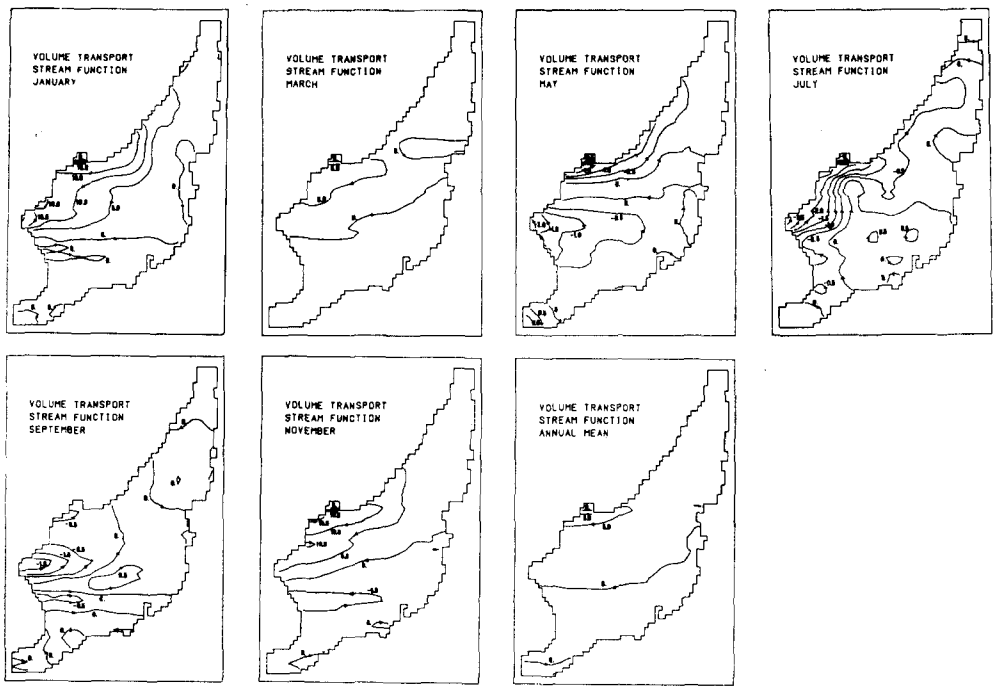

Fig. 9. Volume transport stream function over the Japan Sea computed from the atmospheric pressure. Contour units are 10^6 m^3 sec^{-1}.

Wind stress curl

The distributions of the wind stress curls are shown in Fig 6 and Fig. 7.

(3) In the curl distributions computed from H&L's wind stress data anticyclonic curl is formed in the northern part of the Japan Sea in winter, but its intensity is continually decreased and becomes almost zero in summer (Fig. 6).

(4) In the distributions of the curl deduced from the atmospheric pressure several small scale anticyclonic curls are formed off the southeast coast of Siberia through off the northeast coast of Korea in Winter (Fig. 7). The maximum value is shown off the southeast Siberian coast and 10 times larger than that of H&L in January (Fig. 6 and Fig. 7). Positive values are shown along the Japan side in winter (Fig. 7). The anticyclonic curl in winter is reversed to weak cyclonic in summer in the northwestern part of the Japan Sea (Fig. 7).

Volume transport

Those discrepancies mentioned above are also shown in the volume transport distributions (Fig. 8 and Fig. 9).

(5) In the case of H&L the volume transport stream function shows a broad southward transport pattern over the entire Japan Sea in November through January (Fig. 8). The center of circulation is declined to the northwestern side of the Japan Sea. The amount of volume transport is about 5.0×10^6 m^3 sec^{-1} in winter and almost zero in summer.

(6) In the volume transport stream function computed from the atmospheric pressure it is shown that about 15×10^6 m^3 sec^{-1} of water is transported from off the Siberian coast to off the northeast coast of Korea in January (Fig. 9). On the contrary weak northeastward transport is formed in spring through summer and about 2×10^6 m^3 sec^{-1} in July (Fig. 9).

DISCUSSION

As was noted above, some different features are shown between the two sets of calculations. For the possible

causes of such differences some basic problems can be pointed out such as the sparse input wind stress points of H&L in the calculation of wind stress curl, suitability of the drag coefficient adopted in the present study and calculation of geostrophic wind from the mean atmospheric pressure data. The number of input points in the atmospheric pressure data is more than twice of H&L's wind stress data points in the small grid system (Fig. 2). Moreover, it is reported that the meteorological information on the northwestern region of the Japan Sea has been poorly collected compared with the rest area of the Japan Sea by research vessels or fishing boats (Japan Meteorological Agency, 1972). Considering these facts it is supposed that the wind stress pattern obtained from the atmospheric pressure, especially the finer structure shown in the northwestern part of the Japan Sea, is more reliable than the wind stress distribution pattern obtained from H&L.

The magnitude of the maximum wind stress is about 1.0 dyn cm^{-2} in the distribution of H&L in January but about 3.5 dyn cm^{-2} was obtained in the wind stress distribution computed from the atmospheric pressure. This value of wind stress resulted from the wind speed of about 13 m sec^{-1}. The drag coefficient used here (Heaps, 1965) brings about relatively large value at the higher wind speed compared with the drag coefficients proposed by Wu (1982), Garrett (1977) and Smith (1980). However at the wind speed of 13 m sec^{-1} drag coefficient relationships proposed by Wu (1982) and Garrett (1977) give almost the same wind stress value with the drag coefficient proposed by Heaps (1965). Smith (1980)'s relationship gives less drag coefficient and results in the maximum wind stress of about 3.0 dyn cm^{-2}. But this is still 3 times larger than the maximum wind stress of H&L. Fig. 10a is the monthly mean sea level atmospheric pressure in January used in the present computation. The isobars are parallel to the Korean and Siberian coast and denser in the nearshore region than in the central part of the Japan Sea. From the isobaric pattern it is inferred that strong wind is blowing parallel to the Korean and Siberian coast. It is supposed that the main reason why the different maximum wind stress was obtained in the two sets of wind stress distributions is due to the fact that the relatively large wind speed was computed from the geostrophic wind relationship in the northwestern part of the Japan Sea.

Although the wind stress curl in H&L was computed on the 0.25° square grid system, the resolution is essentially the same as one obtained from the 5° square grid system because the original wind stress data were presented by 5° interval by H&L. According to Saunders (1976) these data spacing could underestimate maximum value in the curl as much as 50%. Considering the Saunders' study the maximum curl in H&L can be corrected to two times of the original value, that is, 4×10^{-8} dyn cm^{-3} in January. However the maximum curl in January computed from the atmospheric pressure is still 5 times larger than the corrected maximum curl of H&L (Fig. 7). It is because of the reason that the maximum wind stress obtained from the geostrophic wind field is about 3.5 times larger than that of H&L. There is the possibility of overestmation of the wind stress shear. It is supposed that the present grid system with the mesh size of 0.25° has brought about the overestimation of the wind stress shear in the computation of the curl from the atmospheric pressure data. But the magnitude of overestimation cannot be accurately estimated without comparing with the computational result obtained by employing the different mesh size.

The presented volume transport stream functions are the results obtained from the various constriction conditions of Sverdrup relationship (Sverdrup, 1947). The inflow and outflow through the southern and northern straits are not considered. So the flow patterns cannot be directly compared with the real circulation in the Japan Sea. In both of analyses broad Sverdrup flow is formed in the central part of the sea and the return flow is considered to form the western boundary current along the northeast coast of Korea. The maximum value in the westernmost streamline corresponds to the transport of western boundary current. In the case of H&L amounts of 5×10^{6} m^{3} sec^{-1} are considered to be transported northward as a boundary current along the northeast continental slope of Korea to off the southeast coast of Siberia in January (Fig. 8). In the transport distribution computed from the atmospheric pressure strong volume transports up to $10-15\times10^{6}$ m^{3} sec^{-1} are considered to flow northward in January from off the Gulf of Yeongheung to off the Siberian southeast coast (Fig. 9). In July through September

waters of about 2×10^6 m^3 sec^{-1} are considered to flow southward as a boundary current along the northeast coast of Korea with discarding the high value in the shallow shelf region(Fig. 9). However, the absolute values of volume transport are not so important because of its dependence on the wind stress curl which was discussed above.

Fig. 10b is the atmospheric pressure distribution from synoptic weather map. It shows quite different feature from the mean pressure pattern of Fig. 10a. It is reported that the cyclones develop in Manchuria in winter or spring and pass through the Japan Sea once a month on the average(Kim, 1972). As a future study it is needed to examine the response of the Japan Sea corresponding to the short term fluctuation of wind stress field together with the incorporation of inflow and outflow of the Tsushima current and of bottom topography.

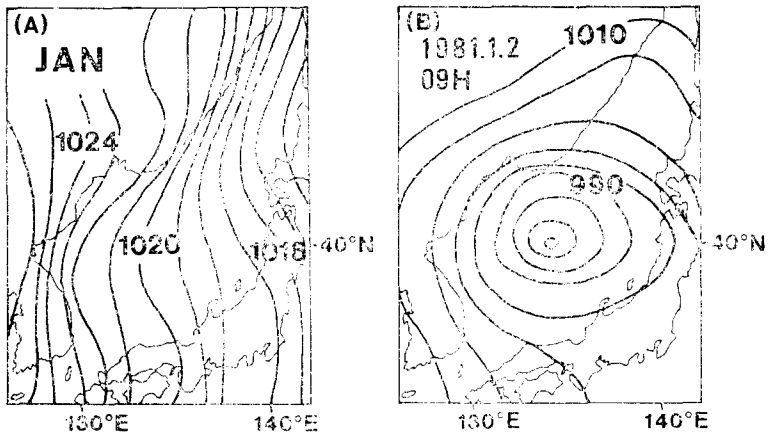

Fig. 10. Surface pressure map. (a) Monthly mean for January. (b) Synoptic chart for 0900 KST 2 January, 1981.

CONCLUSION

This paper has presented a short account of monthly wind stress and wind stress curl distributions in the Japan Sea. The two sets of distributions show strong northwesterly wind stress in winter and weak southwesterly wind stress in summer as a whole. In winter maximum value of wind stress and strong anticyclonic curls are occurred in the northwestern part of the Japan Sea.

The distribution patterns deduced from the sea level atmospheric pressure data show more detailed structure than those from H&L's wind stress data. But the order of magnitude of each distributions is not coincident with each other. The computed volume transport stream functions strongly suggest that the wind stress in winter and summer may generate the boundary current along the northeast coast of Korea.

References

1. Bryan, K.(1963) A numerical investigation of a nonlinear model of a wind-driven ocean. *Journal of Atmospheric Sciences*, 20, 594~606.
2. Bryan, K. and M.D. Cox(1967) A numerical investigation of the oceanic general circulation. *Tellus*, 19, 54~80.
3. Evenson, A.J. and G. Veronis(1975) Continuous representation of wind stress and stress curl over the world ocean. *Journal of Marine Research*, 33, 131~144.
4. Hantel, M.(1972) Wind stress curl the forcing function for oceania motions. In: *Studies in physical oceano-*

graphy, A.H. Gordon, editor, Gordon and Greach, New York, pp. 121～136.

5. Han Y.J. and S.W. Lee(1981) A new analysis of monthly mean wind stress over the global ocean. Climate Research Institute, Report, 26, Oregon State University, Corvallis, 148pp.
6. Hasse, L. and V. Wagner(1971) On the relationship between geostrophic and surface wind at sea. *Monthly Weather Review*, 99, 255～260.
7. Heaps, N.S.(1965) Storm surges on a continental shelf. *Philosophical Transactions of the Royal Society of London*, A257, 351～383.
8. Hellerman, S.(1967) An updated estimate of the wind stress on the world ocean. *Monthly Weather Review*, 95, 607～626. With correction notice in *Monthly Weather Review*, 96, 63～74, 1968.
9. Japan Meteorological Agency(1968) Normals of monthly mean sea level pressure for the northern and southern hemisphere. Technical Report, 61, 171pp.
10. Japan Meteorological Agency(1972) Marine meteorological study of the Japan Sea. Technical Report, 80, 116 pp.
11. Kawabe, M.(1982) Branching of the Tsushima Current in the Japan Sea. Part Ⅱ. Numerical Experiment. *Journal of Oceanographical Society Of Japan*, 38, 183～192.
12. Kim, S.S.(1972) A study on the mechanism of rapid development of cyclones in the area of the Sea of Japan for the spring season. *Journal of Korean Meteoroloigcal Society*, 8, 1～11.
13. Kutsuwada, K. and K. Sakurai(1982) Climatological maps of wind stress field over the North Pacific Ocean. *Oceanographical Magazine*, 32, 25～46.
14. Munk, W.H.(1950) On the wind-driven ocean circulation. *Journal of Meteorology*, 7, 79～93.
15. Smith, S.D. and E.G. Banke(1975) Variation of the sea surface drag coefficient with wind speed. *Quarternary Journary of Royal Meteorological Society*, 101, 665～673.
16. Sounders, P.M.(1976) On the uncertainty of wind stress curl calculations *Journal of Marine Research*, 34, 155～160.
17. Stommel, H.(1948) The westward intensification of wind-driven ocean currents. *Transactions of the American Geophysical Union*, 29, 202～206.
18. Stommel, H.(1965) Summary charts of the mean dynamic topography and current field at the surface of the ocean and related functions of the mean wind stress. In: *Studies on oceanography*, K. Yoshida, editor, University of Washington Press, Seattle, pp. 53～58.
19. Sverdrup, H.U.(1947) Wind-driven currents in a baroclinic ocean; with application to the equatorial currents of the eastern Pacific. *Proceedings of the National Academy of Sciences*, 33, 318～326.
20. Wu, J.(1969) Wind stress and surface roughness at air-sea interface. *Journal of Geophysical Research*, 74, 444～455.
21. Wu, J.(1982) Wind stress coefficients over sea surface from breeze to hurricane. *Journal of Geophysical Research*, 87, 9704～9706.
22. Yoon, J.H.(1982) Numerical experiment on the circulation in the Japan Sea. Part Ⅲ. Formation of the nearshore branch of the Tsushima Current. *Journal of Oceanographical Society of Japan*, 38, 119～124.